Progress In Electromagnetics Research M, Vol. 112, 231–241, 2022

A Miniaturized Dual-Polarized Band Notched Absorber with Low Insertion Loss

Saurabh Sambhav* and Jayanta Ghosh

Abstract—In this study, a novel, low-profile, polarization-insensitive, and compact band-notched absorber is presented. The objective of the proposed work is to design a miniaturized FSS-based band-notch absorber with high angular stability exhibiting strong operational bandwidth of 130.5% (1.7 GHz to 8.09 GHz). The absorber consists of a reflecting band sandwiched between two absorption bands. The absorption bands lie in between 1.7 GHz to 3.75 GHz and 5.65 GHz to 8.09 GHz respectively. The strong reflection band with 1 dB insertion loss lies in the frequency range from 4.25 GHz to 5.12 GHz. The proposed absorber structure comprises multiple layers with a metal sheet at the bottom. Total thickness of the band notch absorber is only $0.064\lambda_L$ (where λ_L is the wavelength corresponding to the lowest frequency of operation). The top layer comprises a modified swastika frame metallic structure loaded with lumped resistors placed on a dielectric substrate. Two air layers, one below the top layer and the other above the bottom metal, are inserted. In between two air layers a dielectric layer with a metallic rectangular ring pattern is positioned. The four-fold symmetrical structure results in polarization insensitive response. The equivalent circuit of the proposed structure is developed for understanding the underlying working principle of band notch absorbers. The surface current distribution has also been studied. The designed absorber is fabricated, and measurements are done in an anechoic chamber. The measured results show good agreement with the simulated ones.

1. INTRODUCTION

There has been an emphasis on radar cross section (RCS) reduction technologies in recent years [1], and many methods have been applied to create or incorporate frequency selective surface-based absorbers into vehicle designs [2]. Aircraft RCS reduction is an important issue that needs to be addressed due to the increased usage of radar systems [3]. Whether it is military operations or other communications, antennas exhibit electromagnetic scattering during their propagation [4]. The term RCS refers to the portion of an electromagnetic signal scattered by an object in all directions away from its source. Recently, the use of composite conductive-magnetic absorbing materials [5] and carbon composites [6] for RCS reduction was demonstrated. Microwave absorbers have been frequently used in many of these applications such as in the reduction of radar cross section, shielding of electromagnetic waves, electromagnetic compatibility, and mobile communication application. Earlier absorber designs were limited to narrow band range. Later the designs were modified for broadband range. A few reported designs used the scattering cancellation technique [7] or polarization conversion method [8] to reduce RCS. Frequency selective surface could provide electromagnetic scattering in the microwave band and reflection at higher frequencies. Frequency Selective Surface (FSS) based absorbers have received significant consideration due to their absorption capability which can reduce RCS as well as electromagnetic interference (EMI) [9]. A few recently reported frequency selective absorbers have either a band transmission property [10] or band-reflecting property [11] along with an absorption

Received 29 June 2022, Accepted 16 August 2022, Scheduled 23 August 2022
* Corresponding author: Saurabh Sambhav (ssambhav.iit@gmail.com).
The authors are with the Department of Electronics and Communication Engineering, National Institute of Technology, Patna, India.

property. A frequency selective surface-based band notch absorber is a frequency selective structure that can selectively absorb and/or reflect electromagnetic energy of specific frequencies [12]. An FSS-based absorbing device that exhibits strong reflection at resonance frequencies and low absorption at nonresonant frequencies can be called a frequency reflector, and these properties make frequency reflectors ideal for RCS reduction and radar-to-radar interference mitigation [13]. For the related purpose, the frequency selective surface based absorber has been investigated in many works [14]. FSS-based advanced radar absorbent coatings can be effective at reducing the RCS of objects, but they are often large and fragile [15]. Some planar frequency absorbers/rasorbers have been reported but have asymmetrical geometry [16]. Lately, frequency selective rasorbers (FSRs) have been reported, which can transmit in-band and absorb out-of-band frequencies having applications in stealth applications and RCS reduction [17]. The absorbers which can operate over a good range of frequencies are very useful in defense sectors and cloaking. However, they are large in size and heavy in weight, so become unsuitable for such operations. Several other methods like nanotubes or pyramidal designed structures have also been reported, but the main issue is their size, maintenance, and cost. A few designs are found to be symmetrical but they are bulky [18]. The polarization insensitivity of the absorber is also one of the critical requirements [19]. Some structures are compact, but they suffer from polarization sensitivity and some from lower fractional bandwidth [20]. Hence, most of the absorbers which were reported earlier were limited in terms of polarization properties or their bandwidth range [21]. If somehow, they managed to have both these major characteristics, then their unit cell insertion loss, size, periodicity, and fractional bandwidth were major issues [22]. Here in this study, a miniaturized, dual-polarized absorber is fabricated which has a fairly high fractional bandwidth along with lower loss and greater angular stability than earlier reported structures. The incorporation of band-notch absorbers not only reduces RCS but also mitigates the co-located radar system's interference effects as they behave as a substrate when being used as a ground plane for the antenna [23]. Since it has both reflective and absorptive properties, the proposed frequency band notch absorber can be a good candidate for RCS reduction.

2. CONCEPTION AND UNIT CELL GEOMETRY

The design of a frequency selective absorber capable of simultaneous absorption/reflection can be a complex one. The antenna structures generally have a ground plane which has the property of reflection. The reflection property can be utilized using a band-stop filter as shown in Figure 1(a), but the addition of the absorption property to the reflection property can help simultaneous RCS reduction of the antennas. The combined property of absorption and reflection is shown in Figure 1. Thus, these absorbers can behave as a ground plane in the operating range of the antenna and help in antenna operation. The proposed band notch absorber absorbs the out-of-band region of the incoming wave and helps in the reduction of RCS. To address all these requirements, we have designed a band-notch structure that is novel, compact, simple, and dual polarized.

The unit cell geometry of the proposed frequency selective band notch absorber is shown in Figure 2. The unit cell of the proposed band notch absorber consists of a modified swastika frame structure as an upper layer laden with resistors (R) of 85 ohms embedded on an FR4 substrate, thus acting as a lossy layer as shown in Figure 2(a). Here, lumped resistors are used as lossy material which helps in achieving good out-of-band absorption. FR4 material with 0.2 mm thickness has been used as a substrate whose relative permittivity and dielectric loss tangent are 4.4 and 0.02, respectively. The middle layer consists of another substrate layer of the same FR4 material with a metallic square loop patterned at the upper surface as shown in Figure 2(b). The bottom layer is a ground plane. So, the proposed band notch absorber is a three-layer structure with two air layers sandwiched in between these three layers as shown in Figure 2(c). Figure 2(d) portrays the side view of the band-notch absorber. The proposed absorber has been simulated using HFSS software. The absorbers are periodic arrangements of unit cells, and periodicity in simulation is achieved by imposing periodic boundary conditions (master and slave) in the unit cell. The Floquet port excitation is provided to the unit cell. Optimal dimensions of the proposed absorber are as follows: $p = 15\,\text{mm}$, $a = 14\,\text{mm}$, $b = 0.6\,\text{mm}$, $c = 12.2\,\text{mm}$, $d = 6\,\text{mm}$, $e = 1\,\text{mm}$, $w_1 = 1.25\,\text{mm}$, $w_2 = 1.5\,\text{mm}$, $l_1 = 8.25\,\text{mm}$, $l_2 = 6.25\,\text{mm}$, $l_3 = 4.25\,\text{mm}$, $l_4 = 6.25\,\text{mm}$, $t_1 = 0.2\,\text{mm}$, $t_2 = 0.2\,\text{mm}$, $t_3 = 6\,\text{mm}$, $t_4 = 11.4\,\text{mm}$, $t_5 = 5\,\text{mm}$.

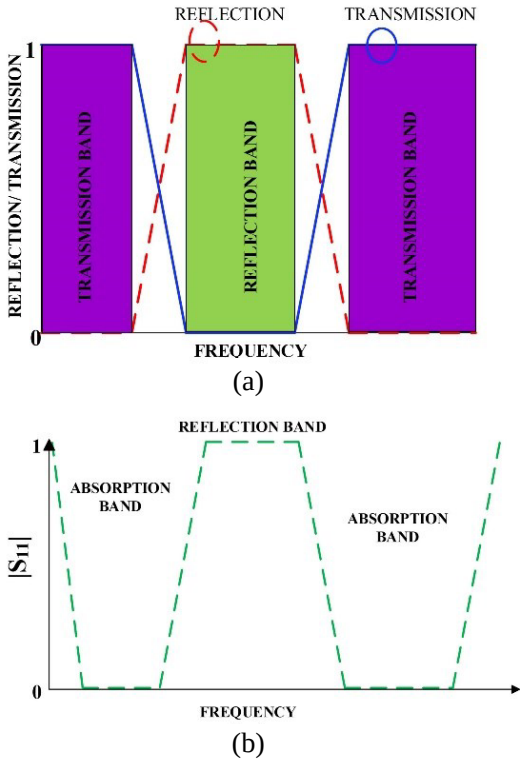

Figure 1. (a) Reflection coefficient profile of band stop filter, (b) reflection coefficient profile of band notch absorber.

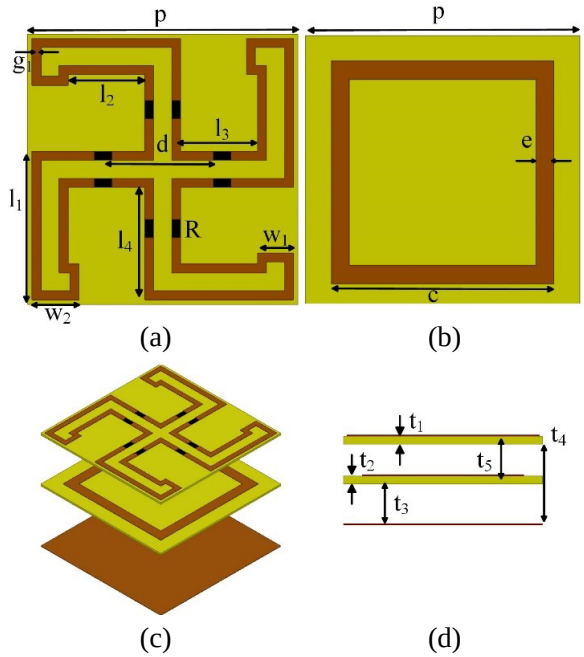

Figure 2. Schematic of proposed Unit cell structure, (a) top layer, (b) middle layer, (c) isometric view of band-notch absorber, (d) side view of the band-notch absorber.

For an ideal absorber, there should not be any transmitted or reflected wave, i.e., S_{11} and S_{21} should be zero to maximize absorption. The same cannot be applied to the band notch absorber as the total frequency range for the band notch absorber is divided into three bands, i.e., lower absorption band (f_1), reflection band (f_2), and upper absorption band (f_3). For band notch absorber at f_1 and f_3, S_{11} and S_{21} should be zero, but at f_2, S_{11} should be 1 whereas S_{21} should be zero. In practical designs, S_{11} less than -10 dB is considered for absorber design. The simulated reflection coefficient and absorptivity of the proposed band-notch absorber are shown in Figure 3. The band notch absorber works in the frequency range of 1.7 GHz to 8.09 GHz. The lower absorption band occurs from 1.7 GHz to 3.75 GHz, and the upper absorption band is achieved from 5.65 GHz to 8.09 GHz. 1 dB reflection band range is 4.25 GHz to 5.12 GHz.

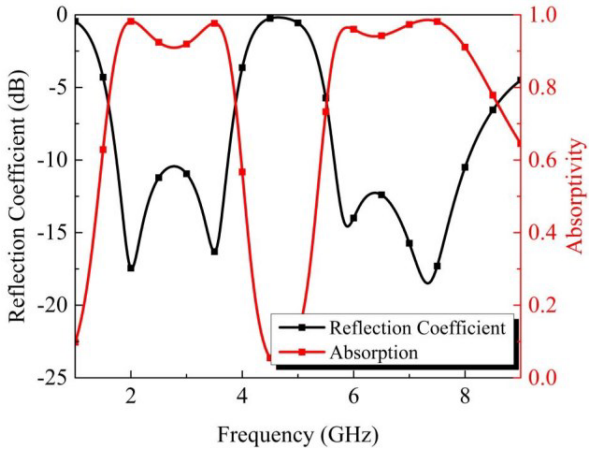

Figure 3. Simulated reflection coefficient and absorptivity of the proposed band-notch absorber.

As discussed earlier, the band-notch absorber is a three-layered structure, where the top layer helps in obtaining a wide absorption band; the middle layer consisting of square loop geometry helps in obtaining a selective reflection band; and the bottom ground plane helps in restricting the transmission. Both lossy (top) and lossless (middle) frequency selective surfaces must be aligned and tuned in such a way that a selective reflection band with low insertion loss is obtained between two absorption bands. Thus, the overall geometry results in wide-band absorption characteristics along with a middle reflection band. As the middle layer is introduced, the visible change in response can be seen. The absorption bands become wider along with a steep reflection band. The effect of the middle layer can be observed in Figure 4 where we can see a narrow reflection band because of this middle band. Thus, to obtain a wide-band absorption range and a narrow band-notch range, a square loop geometry-based middle layer is introduced between the top and bottom layers. The final structure shows good response, and a flat reflection band is found in between two wide absorption bands.

The lumped resistor (R) value has been varied to get an optimized operating bandwidth and is shown in Figure 5. A significant change in absorption bands is observed whereas reflect band response is unaffected by the change in resistance values. The optimum response is achieved when resistance (R) is 85 ohms. The thickness of both air layers has also been optimized. Figure 6 shows the variation in reflection coefficient with respect to variation in air spacer thickness t_5. The optimal thickness is found to be 5 mm. Figure 7 depicts that the proposed absorber shows the same response with different polarization angles because the four-fold symmetric nature of the structure adds to the polarization insensitivity to the structure. The nature of the incidence of the electromagnetic wave also plays an important role in understanding the concept of the reflection coefficient.

It is seen that the proposed absorber displays almost the same results with incident angle variation. Equation (1) and Equation (2) represent the reflection coefficients for perpendicular polarization (TE)

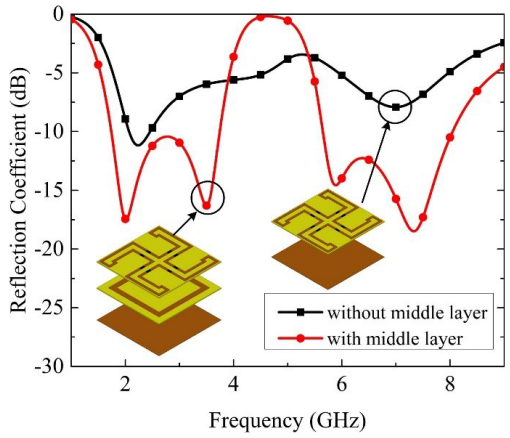

Figure 4. Variation in reflection coefficient of the band-notch absorber with and without the middle layer.

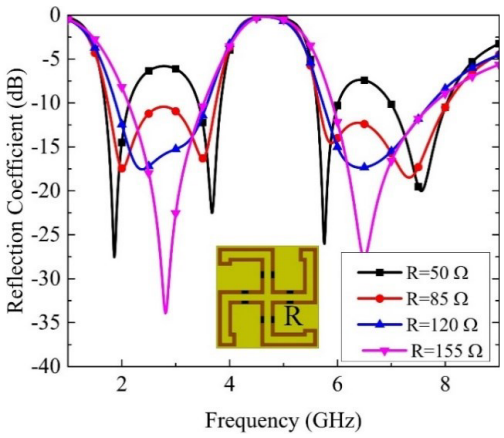

Figure 5. Variation in reflection coefficient with variation in resistance (R) embedded on the top metal layer.

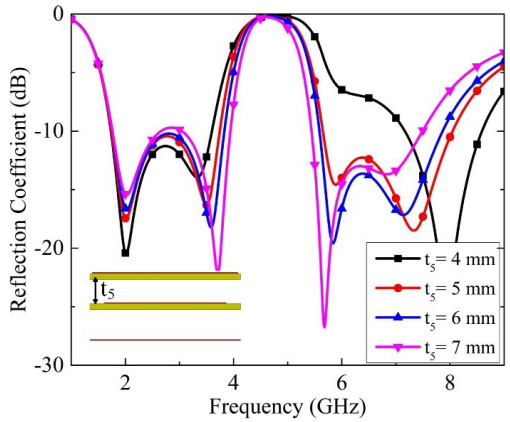

Figure 6. Variation in reflection coefficient with variation in air spacer thickness.

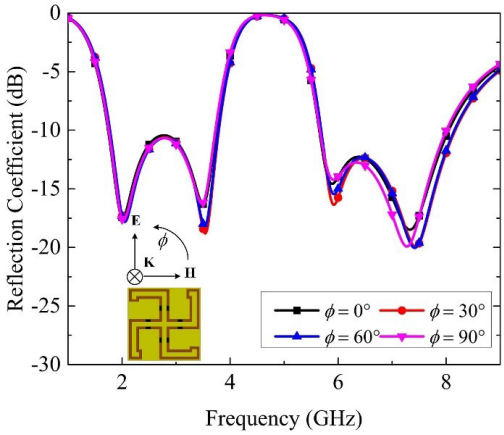

Figure 7. Reflection coefficients for different polarization angles for band-notch absorber.

and parallel polarization (TM) under oblique incidence situation respectively [13].

$$\Gamma_{\perp}(w) = \frac{z(w)\cos\theta_i - z_o\cos\theta_t}{z(w)\cos\theta_i + z_o\cos\theta_t} \tag{1}$$

$$\Gamma_{\parallel}(w) = \frac{z(w)\cos\theta_t - z_o\cos\theta_i}{z(w)\cos\theta_t + z_o\cos\theta_i} \tag{2}$$

From the above equations, it is seen that as the incident angle changes, the reflection coefficient changes (here, θ_t and θ_i are the transmission angle and incident angle, respectively). The reflection coefficient increases, and corresponding absorptivity decreases when an electromagnetic wave is an incident obliquely on the surface. For perpendicular polarization, the magnetic field and propagation direction of electromagnetic wave rotate at various incidences keeping the electric field constant. For parallel polarization, the electric field and electromagnetic wave propagation direction rotate at various incidence angles keeping the magnetic field constant. The miniaturization and low profile of the structure help in making the structure angularly stable to the oblique incidence angles. The oblique incidence responses for TE and TM polarizations are shown in Figure 8 and Figure 9, respectively. The structure is stable with no occurrence of grating lobes up to 40° for both TE and TM polarizations, but the response degrades after 40° for TM polarization.

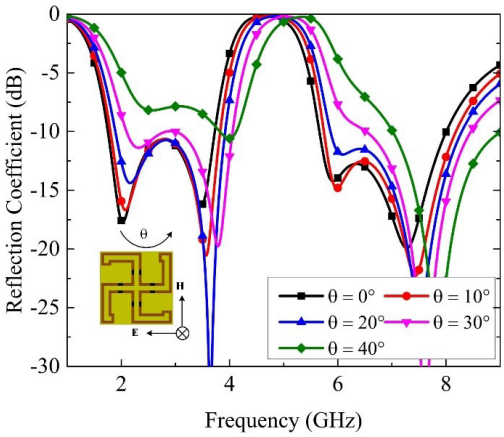

Figure 8. Reflection coefficients for oblique incidence in case of TE Mode.

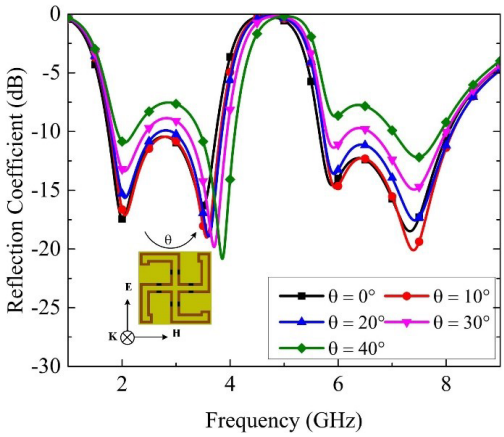

Figure 9. Reflection coefficients for oblique incidence in case of TM Mode.

3. ABSORPTION MECHANISM OF PROPOSED ABSORBER

To comprehend the behavior of the band notch absorber, an equivalent electrical circuit is proposed as shown in Figure 10. The upper layer is modeled with the arrangement of series and parallel circuits of resistive and reactive elements. A ground plane is required at the rear side of the structure to confirm zero transmission for the complete band. To introduce a reflection band, the middle layer with a square loop is employed and has been modeled as a series combination of L-C circuits between the top and bottom layers. The values of all the lumped components used in the circuit are as follows: $R_{1t} = 270\,\text{ohm}$, $L_{1t} = 7.12\,\text{nH}$, $C_{1t} = 0.23\,\text{pF}$, $L_{2t} = 3.66\,\text{nH}$, $C_{2t} = 0.281\,\text{pF}$, $C_{1b} = 0.08\,\text{pF}$ and $L_{1b} = 10.68\,\text{nH}$. Good agreement between the reflection coefficients obtained from simulation and proposed circuit model is observed as shown in Figure 11.

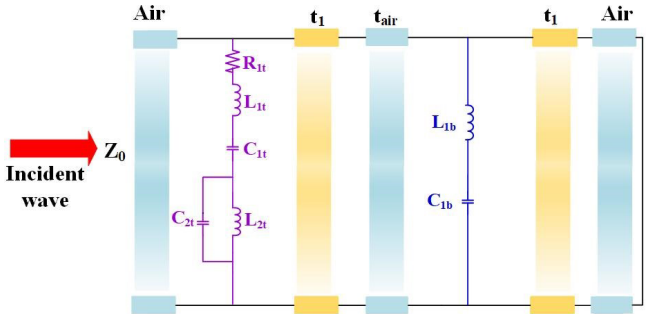

Figure 10. The Equivalent circuit for the proposed FSS-based band-notch absorber.

The absorption is achieved due to the series resonance by the series RLC along with the capacitive or inductive behavior of the parallel LC circuit. The reflective behavior comes into the picture because of the parallel LC circuit which behaves as an open circuit at resonance and allows the incoming wave to pass through the top layer. When the incoming wave reaches the middle layer (band-stop filter), it gets reflected and hence creates a notch at resonance. Thus, the combination of serial and parallel LC circuits is required to obtain a reflection band along with absorption bands. The reactive elements (inductance and capacitance) can be calculated using Equation (3) & Equation (4) respectively [13].

$$L = \mu_o \mu_{eff} \frac{p}{2\pi} \ln \frac{1}{\sin \frac{s\pi}{2p}} \tag{3}$$

$$C = \varepsilon_O \varepsilon_{eff} \frac{2p}{\pi} \ln \frac{1}{\sin \frac{g_1 \pi}{2p}} \tag{4}$$

The absorber response can also be explained by analyzing the surface current distribution which is displayed in Figure 12. The top layer, i.e., lossy layer, is excited at the absorption frequencies 2 GHz and 6.8 GHz and causes the current to flow through the resistors, thus giving wide absorption bands. The lossless layer, i.e., middle layer, is found to be excited at the frequency around 4.9 GHz. So, it is concluded that the wide absorption bandwidth is because of lumped resistors present at the top layer whereas the middle layer contributes to the selectivity of the reflective band.

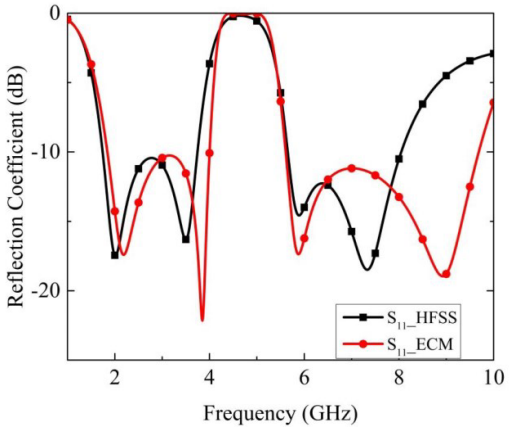

Figure 11. Comparison of results obtained through HFSS and Equivalent circuit model (ECM).

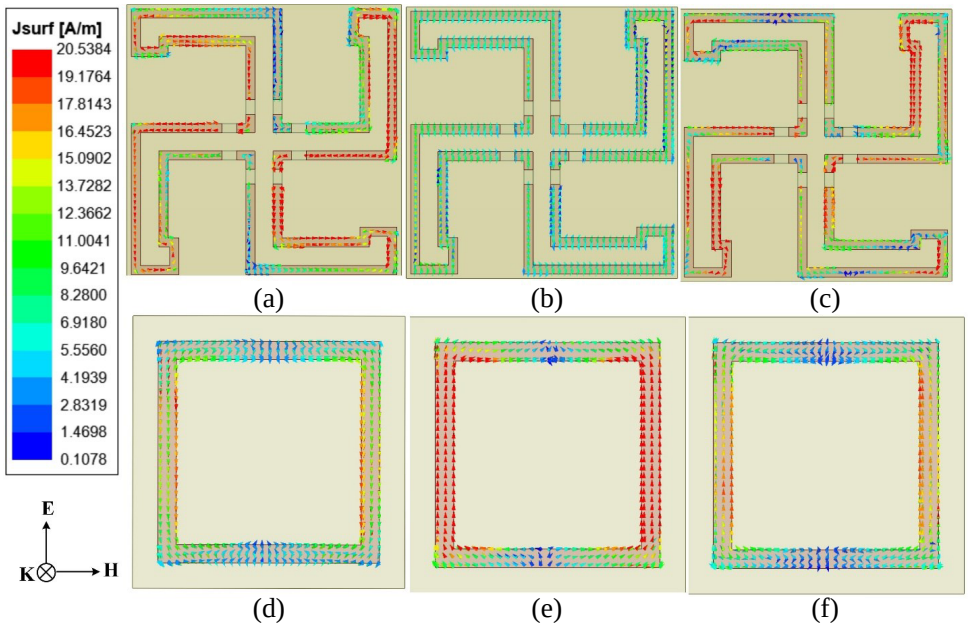

Figure 12. Surface current distribution on the top layer at (a) 2 GHz, (b) 4.9 GHz, (c) 6.8 GHz, and on the middle layer at (d) 2 GHz, (e) 4.9 GHz, and (f) 6.8 GHz.

4. FABRICATION AND MEASUREMENT OF PROPOSED ABSORBER

To validate the working of our simulated designs, a prototype of both the band notch and band transmitting absorber was prepared. All the different layers were prepared individually using printed

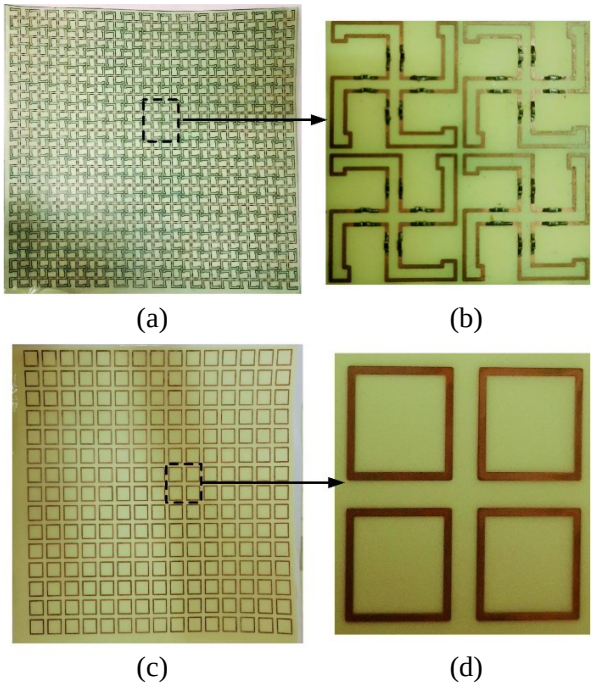

Figure 13. Fabricated sample, (a) top layer of band-notch absorber, (b) enlarged view of middle layer, (c) middle layer of band-notch absorber, (c) enlarged view of the top layer, (d) enlarged view of the middle layer.

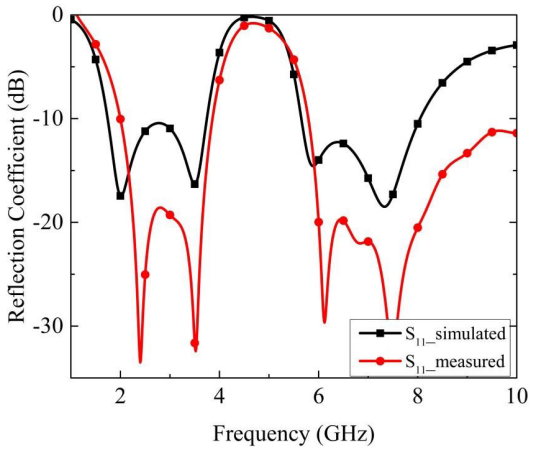

Figure 14. Comparison of reflection coefficient between the simulated and measured results of proposed band notch absorber.

circuit board technology and then assembled for measurement. The lumped resistors are soldered across the gaps. The air spacer between the different layers was maintained using flexible foams. In the proposed absorber, there are two air layers that are realized with a foam layer. The foam layer is used because the dielectric constant of the foam layer is approximately equal to 1. Four small pieces of foam layer with the required height are kept at four corners to realize the air layer. This is done to keep the dielectric constant of the layer equal to almost one (1). The foam layer used to realize the air layer in the proposed absorber is ROHACELL 31 HF of dielectric constant 1.04 and loss tangent 0.0017 [24–26]. FR4 of thickness 0.2 mm was used as a substrate for the different layers. Photos of the fabricated structure are shown in Figure 13. The prototypes of the absorbers were measured in an anechoic chamber using free space measurement techniques. For carrying out the reflection coefficient

measurement of the two structures, two identical horn antennas were kept side by side, and the prototype was kept at a distance of 210 mm. The normalization was done with a copper plate of the same area as the prototype. For measuring the transmission coefficient, the prototype was kept in between the two antennas linearly. The normalization was carried out with the free space or nothing in between the two antennas. The simulated reflection coefficient and measured reflection coefficient of the band notch absorber are plotted in Figure 14. The graph shows that there is a decent agreement between measured and simulated results. The reflection coefficient has better results than the simulated results which might be attributed to the value of lumped resistors used during soldering. The performance of the proposed work is compared with that of other state-of-the-art works in Table 1 for the proposed band-notch absorbers. The absorber is found to be good in terms of fractional bandwidth, thickness, and insertion loss. Also, they are polarization insensitive and angularly stable. In terms of unit cell size and periodicity, they are very optimal and compact.

Table 1. Comparison of the proposed band notch absorber with earlier published works.

Ref. No.	**IL (dB)/ Frequency (GHz)**	**Relative Thickness**	**Fractional Bandwidth**	**Unit Cell Size (mm)**	**Periodicity (λ_L)**	**Angular Stability (Degrees)**	**Polarization Insensitivity**
9	N.A.	0.104	107.7	16	0.219	30	No
10	−0.12/3.5	0.089	111.6	25	0.170	45 TE/ 30 TM	Yes
11	−0.33/5	0.084	127.52	19.5	0.137	45	Yes
14	−0.45/10	0.105	115.2	10.2	0.18	30	Yes
Our Work	**−0.17/4.9**	**0.064**	**130.5**	**15**	**0.08**	**40**	**Yes**

5. CONCLUSIONS

A novel, miniaturized, wide-band, and dual-polarized frequency selective surface-based band-notch absorber has been developed with characteristics like very low insertion loss, good angular stability, and high fractional bandwidth. The proposed band-notch absorber exhibits wide-band absorption in two distinct absorption bands from 1.7 GHz to 3.75 GHz and from 5.65 GHz to 8.09 GHz, whereas a reflective behavior of 1 dB is obtained from 4.25 GHz to 5.12 GHz. This shows strong fractional absorption bandwidth of 130.5% (above 90% absorption). The analysis of the proposed absorber is projected using different parametric variations, surface current distribution, and equivalent circuit model. The proposed geometry is only $0.064\lambda_L$ thick (where λ_L corresponds to the wavelength at a lower frequency). It is found that the proposed work is much miniaturized and has high fractional bandwidth operating in lower frequency bands. The proposed design can be a good contender for industries where there is a demand for band-selective notch absorbers and also could meet the band requirements of modern sophisticated surveillance radars.

REFERENCES

1. Ling, H., R.-C. Chou, and S.-W. Lee, "Shooting and bouncing rays: Calculating the RCS of an arbitrarily shaped cavity," *IEEE Transactions on Antennas and Propagation*, Vol. 37, 194–205, 1989.
2. Costa, F. and A. Monorchio, "A frequency selective radome with wideband absorbing properties," *IEEE Transactions on Antennas and Propagation*, Vol. 60, 2740–2747, 2012.

3. Paquay, M. H. A., J. C. Iriarte, I. Ederra, R. Gonzalo, and P. de Maagt, "Thin amc structure for radar cross-section reduction," *IEEE Transactions on Antennas and Propagation*, Vol. 55, 3630–3638, 2007.
4. Iriarte Galarregui, J. C., A. Tellechea Pereda, J. L. M. de Falcón, I. Ederra, R. Gonzalo, and P. de Maagt, "Broadband radar cross-section reduction using AMC technology," *IEEE Transactions on Antennas and Propagation*, Vol. 61, 6136–6143, 2013.
5. Zhou, P., L. Huang, J. Xie, D. Liang, H. Lu, and L. Deng, "A study on the effective permittivity of carbon/pi honeycomb composites for radar absorbing design," *IEEE Transactions on Antennas and Propagation*, Vol. 60, 3679–3683, 2012.
6. Zhuang, Y., G. Wang, Q. Zhang, and C. Zhou, "Low-scattering tri-band metasurface using combination of diffusion, absorption and cancellation," *IEEE Access*, Vol. 6, 17306–17312, 2018.
7. Zheng, Q., C. Guo, J. Ding, and G. A. E. Vandenbosch, "A broadband low-rcs metasurface for CP patch antennas," *IEEE Transactions on Antennas and Propagation*, Vol. 69, 3529–3534, 2021.
8. Ghaneizadeh, A., M. Joodaki, J. Börcsök, A. Golmakani, and K. Mafinezhad, "Analysis, design, and implementation of a new extremely ultrathin 2-d-isotropic flexible energy harvester using symmetric patch fss," *IEEE Transactions on Microwave Theory and Techniques*, Vol. 68, 2108–2115, 2020.
9. Kiani, G. I., K. L. Ford, K. P. Esselle, A. R. Weily, and C. J. Panagamuwa, "Oblique incidence performance of a novel frequency selective surface ab sorber," *IEEE Transactions on Antennas and Propagation*, Vol. 55, 2931–2934, 2007.
10. Mei, P., X. Q. Lin, J. W. Yu, and P. C. Zhang, "A band-notched absorber designed with high notch-band-edge selectivity," *IEEE Transactions on Antennas and Propagation*, Vol. 65, 3560–3567, 2017.
11. Han, Y., L. Zhu, Y. Chang, and B. Li, "Dual-polarized bandpass and band-notched frequency-selective absorbers under multimode resonance," *IEEE Transactions on Antennas and Propagation*, Vol. 66, 7449–7454, 2018.
12. Sharma, A., S. Ghosh, and K. V. Srivastava, "A polarization-insensitive band-notched absorber for radar cross section reduction," *IEEE Antennas and Wireless Propagation Letters*, Vol. 20, 259–263, 2021.
13. Strifors, H. and G. Gaunaurd, "Scattering of electromagnetic pulses by simple-shaped targets with radar cross section modified by a dielectric coating," *IEEE Transactions on Antennas and Propagation*, Vol. 46, 1252–1262, 1998.
14. Han, Y., W. Che, X. Xiu, W. Yang, and C. Christopoulos, "Switchable low-profile broadband frequency-selective rasorber/absorber based on slot arrays," *IEEE Transactions on Antennas and Propagation*, Vol. 65, 6998–7008, 2017.
15. Ding, Y., M. Li, J. Su, Q. Guo, H. Yin, Z. Li, and J. Song, "Ultrawideband frequency-selective absorber designed with an adjustable and highly selective notch," *IEEE Transactions on Antennas and Propagation*, Vol. 69, 1493–1504, 2021.
16. Li, B. and Z. Shen, "Wideband 3d frequency selective rasorber," *IEEE Transactions on Antennas and Propagation*, Vol. 62, 6536–6541, 2014.
17. Omar, A., Z. Shen, and H. Huang, "Absorptive frequency-selective reflection and transmission structures," *IEEE Transactions on Antennas and Propagation*, Vol. 65, 6173–6178, 2017.
18. Chen, Q., S. Yang, J. Bai, and Y. Fu, "Design of absorptive/transmissive frequency-selective surface based on parallel resonance," *IEEE Transactions on Antennas and Propagation*, Vol. 65 4897–4902, 2017.
19. Zhang, Y., B. Li, L. Zhu, Y. Tang, Y. Chang, and Y. Bo, "Frequency selective rasorber with low insertion loss and dual-band absorptions using planar slotline structures," *IEEE Antennas and Wireless Propagation Letters*, Vol. 17 633–636, 2018.
20. Deng, T., Y. Yu, Z. Shen, and Z. N. Chen, "Design of 3-d multilayer ferrite-loaded frequency-selective rasorbers with wide absorption bands," *IEEE Transactions on Microwave Theory and Techniques*, Vol. 67, 108–117, 2019.
21. Han, T., K. Wen, Z. Xie, and X. Yue, "An ultra-thin wideband reflection reduction metasurface based on polarization conversion," *Progress In Electromagnetics Research*, Vol. 173, 1–8, 2022.

22. Shang, Y., Z. Shen, and S. Xiao, "On the design of single-layer circuit analog absorber using double square-loop array," *IEEE Transactions on Antennas Propagation*, Vol. 61, No. 12, 6022–6029, Dec. 2013.
23. Sheokand, H., S. Ghosh, G. Singh, M. Saikia, K. V. Srivastava, J. Ramkumar, and S. A. Ramakrishna, "Transparent broadband metamaterial absorber based on resistive films," *Journal of Applied Physics*, Vol. 122, No. 10, 105105, 2017.
24. Sambhav, S., J. Ghosh, and A. K. Singh, "Ultra-wideband polarization insensitive thin absorber based on resistive concentric circular rings," *IEEE Transactions on Electromagnetic Compatibility*, Vol. 63, No. 5, 1333–1340, Oct. 2021.
25. Singh, G., A. Sharma, and S. Ghosh, "A broadband multilayer circuit analog absorber using resistive ink," *Microwave Optical Technology Letters*, Vol. 63, 322–328, 2020.
26. Malik, S., M. Saikia, A. Sharma, G. Singh, J. Ramkumar, P. K. Mishra, and K. V. Srivastava, "Design and analysis of polarization-insensitive broadband microwave absorber for perfect absorption," *Progress In Electromagnetics Research M*, Vol. 104, 213–223, 2021.